An Initial Vibro-Acoustic Model for Predicting Electric Motor Noise

Greg Busch, Jordan Cluts, Brenda Henderson, and Lennart Hultgren

NASA Glenn Research Center

October 9, 2024

Work is supported by the Revolutionary Vertical Lift Technology Project

RVLT.23.02.L372	**Initial Vibro-Acoustic Model for Outrunning kW Class Electric Motors**	**12/31/24**

RVLT GRC Acoustics: Electric Motor Noise

Problem: There is limited information available in literature about electric motor noise in aerospace systems and its potential impact on AAM noise. No widely-available tools to assist engineers in predicting electric motor noise and inform design decisions for low-noise AAM platforms.

Objective: Develop a modeling tool with the capability to predict noise generated by electric motors with reasonable accuracy for conceptual design studies.

Methodology: Break down the modeling effort into three distinct, but connected, sub-efforts focusing on the electromagnetic forcing system (Busch), the mechanical vibration system (Cluts) and the acoustic propagation (Henderson). Initial focus of modeling tool will be on outrunner electrical motors with permanent magnets (PM) up to 4kW.

Initial Focus of Electric Motor Noise Tool

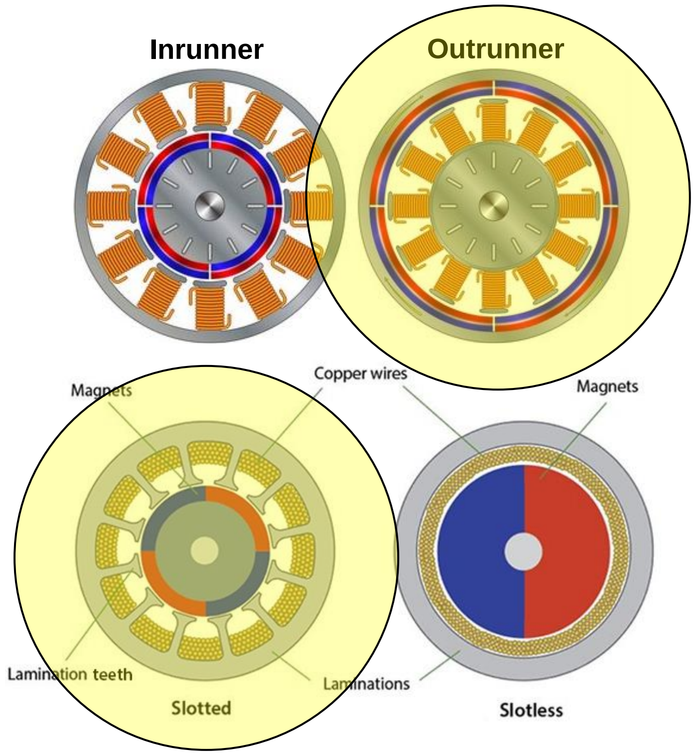

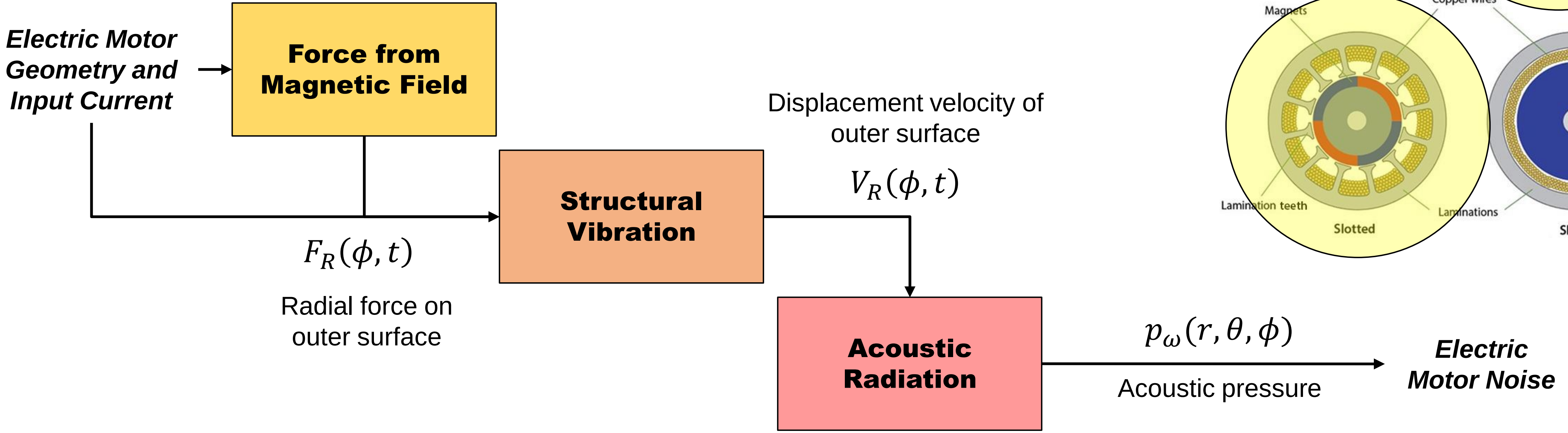

Electric Motor Noise Modeling Process

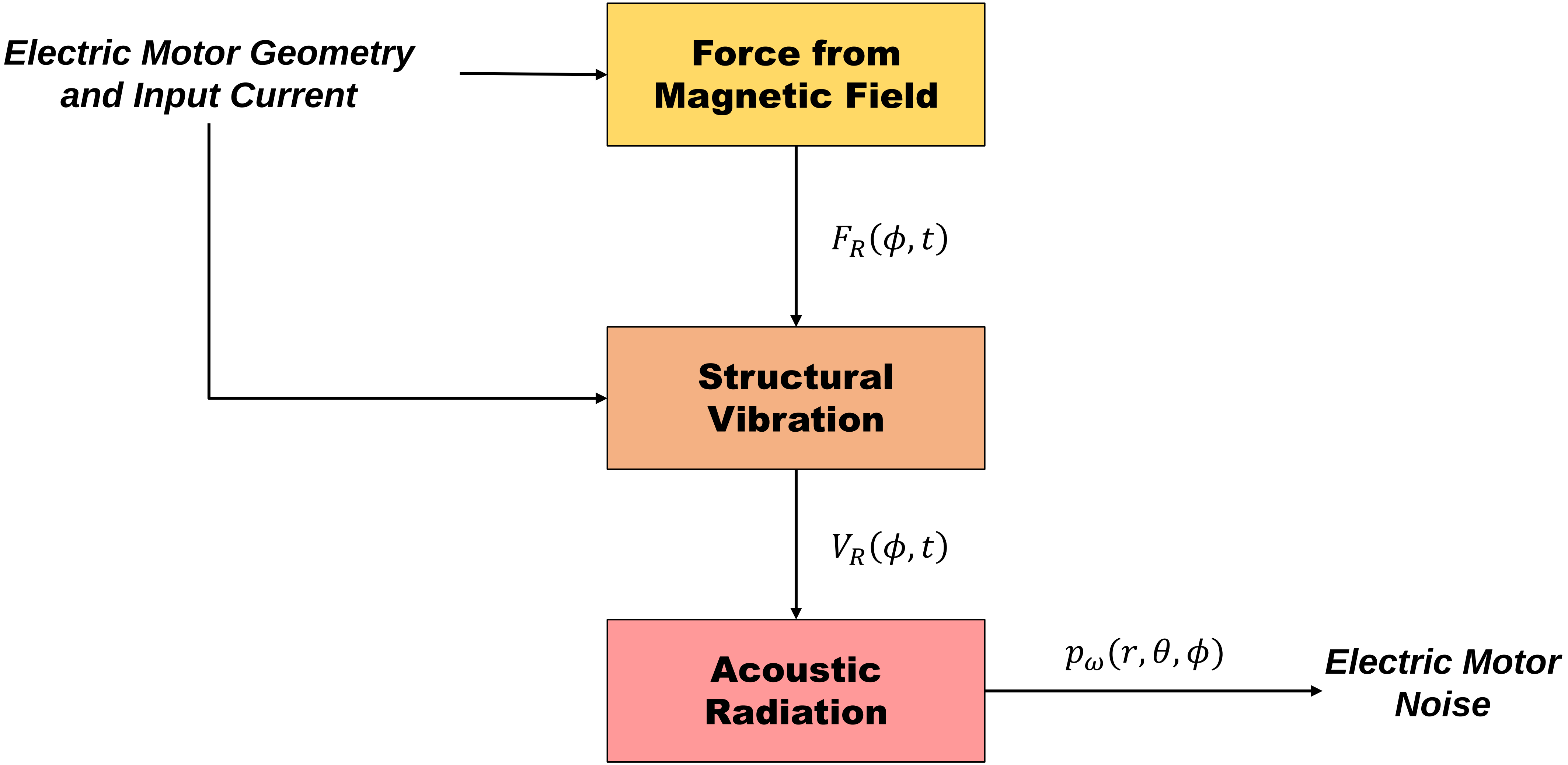

Electric Motor Noise Modeling Process

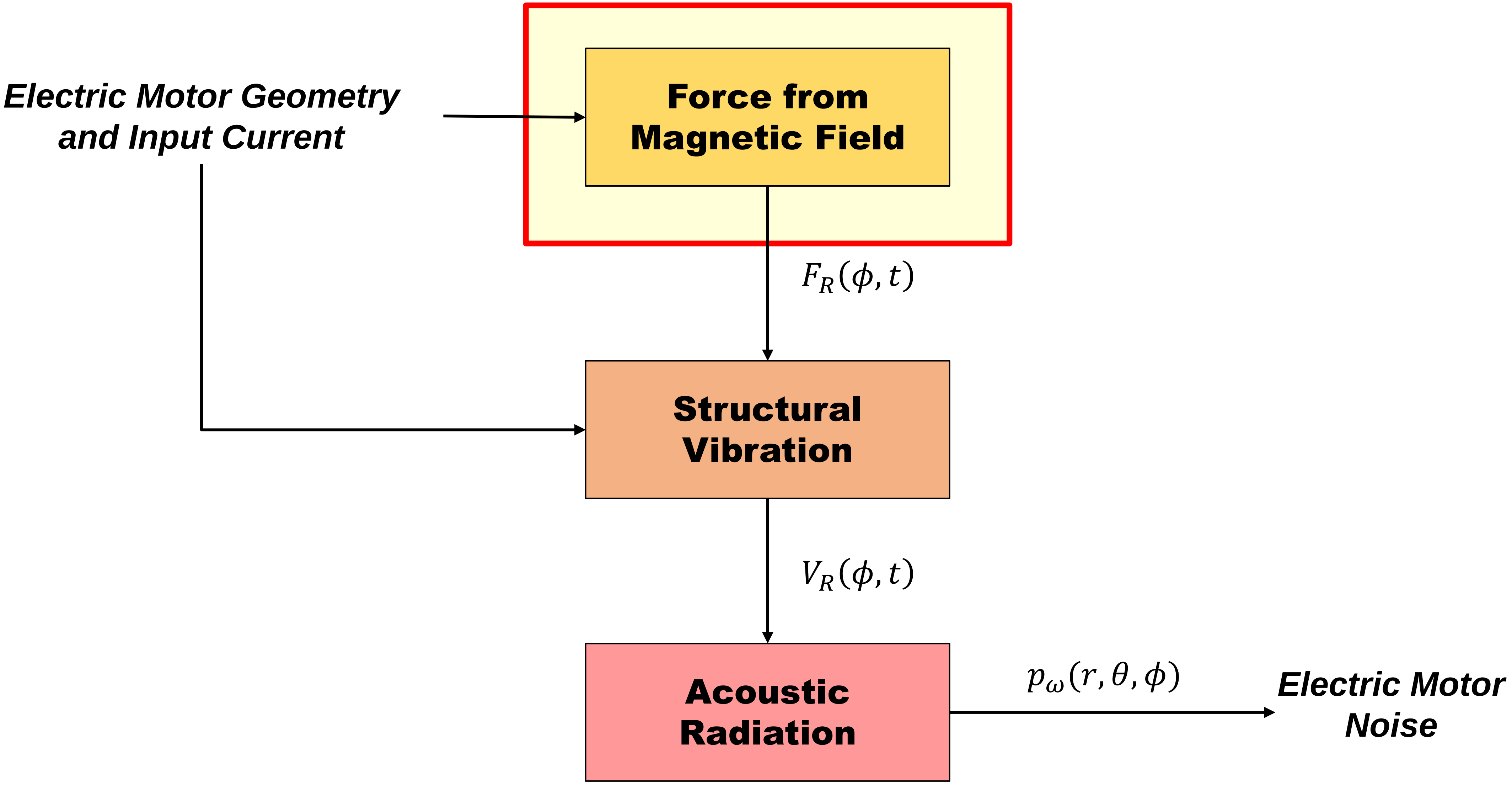

Electric Motor Noise Theory

Pressure from Magnetic Field

- Radial force in terms of radial pressure

$$F_R(\phi,t) = \frac{1}{2b}\int p_R\,dz$$

- Radial pressure is obtained from Maxwell's stress tensor

$$p_R(\phi,t) = \frac{1}{2\mu_o}\left[B_R^2(\phi,t) - B_T^2(\phi,t)\right]$$

small - ignore

B = magnetic flux density

μ_o= magnetic recoil permeability = constant

$B_T \ll B_R$

Stator (windings / armature)

$$B_R = B_{R,PM} + B_{R,W}$$

Rotor (permanent magnet)

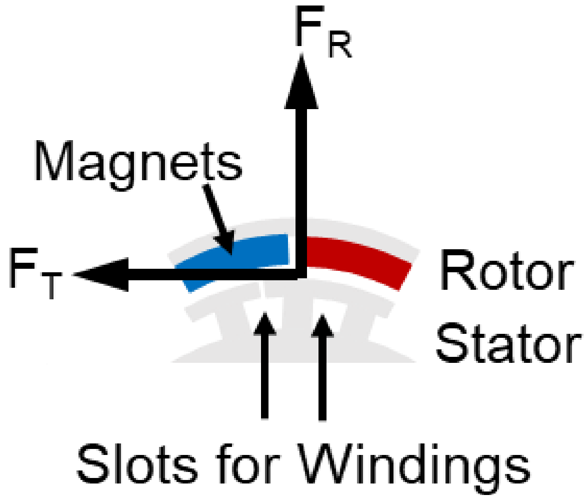

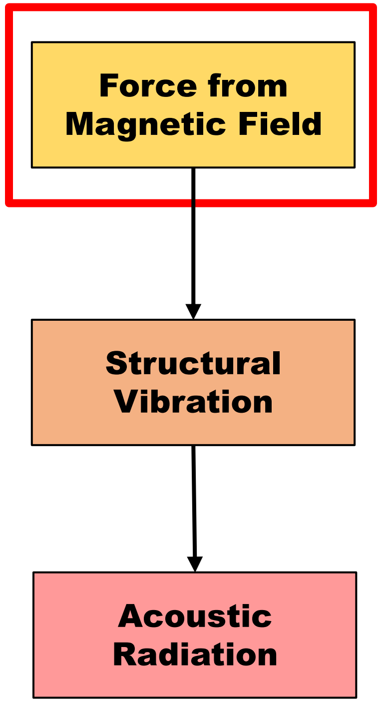

- Resulting radial pressure on outer surface (rotor in this case)

$$p_R(\phi,t) \approx \frac{1}{2\mu_o}\left[B_{R,PM}^2(\phi) + 2B_{R,PM}(\phi)B_{R,W}(\phi,t) + B_{R,W}^2(\phi,t)\right]$$

Rotor Field | Rotor-Stator Interaction | Stator Field

5

Electromagnetic Forcing Function (EMFF) Method Overview

- Goal to compute the magnetic flux density in the radial direction (B_R), and use this with the Maxwell relations to calculate the radial pressure distribution, at a fixed radial distance of the motor shell outer surface

- B_R is broken down into three separate terms that are calculated separately, at a fixed outer radius

  I: $B_{R,PM}(\phi)$ - The contribution of the permanent magnet field

  II: $B_{R,W}(\phi, t)$ - The contribution of the current running through the armature windings

  III: $\lambda(\phi, t) \sim B_{R,PM}(\phi)\ B_{R,W}(\phi, t)$ - The effect of slotting on the relative permeance of the motor system (how easily magnetic flux passes through)

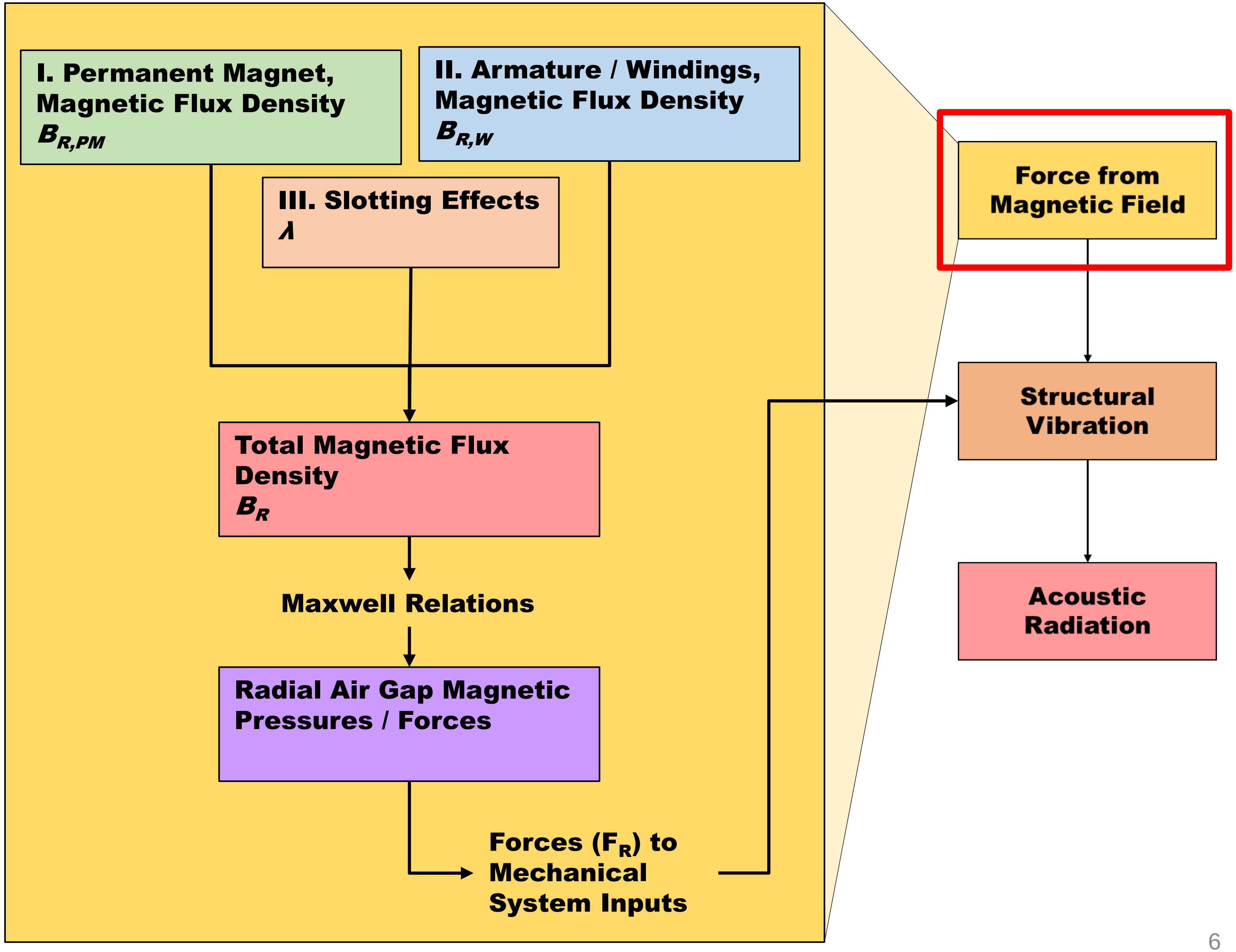

EMFF Part I: Magnetic Flux Density of PM Field

- The relationship between magnetic flux density and magnetic field strength can be written for two separate regions: inside the permanent magnets, and outside the permanent magnets

$$Outside\ of\ PM \qquad \vec{B}_I = \mu_0 \vec{H}_I$$

Where $\vec{H}$ is the magnetic field strength, μ_0 is the recoil permeability, μ_r is the relative recoil permeability

- Since target is the motor acoustics that result from the structural vibration of the motor shell, we can focus our tool on calculating the magnetic flux density outside of the PM only - the magnetic flux density inside the PM does not contribute to the electromagnetic forces on the shell

- Outrunner electric motor with 3-phase windings, this results in an equation that can be numerically evaluated:

$$B_{R,PM}(r,\phi) = \sum_{n=1,3,5,\ldots}^{\infty} \frac{(-\mu_0 M_n)}{\mu_r} \frac{np}{(np)^2-1} \left\{ \frac{(np-1)\left(\frac{R_m}{R_r}\right)^{2np} + 2\left(\frac{R_m}{R_r}\right)^{np-1} - (np+1)}{\frac{\mu_r+1}{\mu_r}\left[1-\left(\frac{R_s}{R_r}\right)^{2np}\right] - \frac{\mu_r-1}{\mu_r}\left[\left(\frac{R_s}{R_m}\right)^{2np} - \left(\frac{R_m}{R_r}\right)^{2np}\right]} \right\} \left[\left(\frac{r}{R_m}\right)^{np-1} + \left(\frac{R_s}{R_m}\right)^{np-1}\left(\frac{R_s}{r}\right)^{np+1}\right] \cos(np\phi)$$

Where p is the number of pole pairs, M_n is the magnetization amplitude, r is radius, R_s is the stator radius, and R_m is the magnet radius – and is assessed for our case at $r = R_s + air\ gap\ length + magnet\ thickness$, which is the outer shell surface

Example output of magnetic flux density in airgap due to PM field

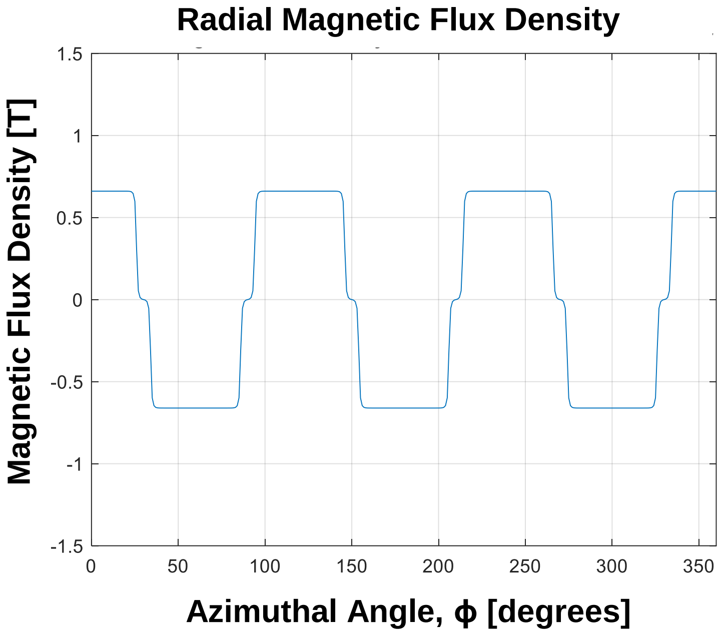

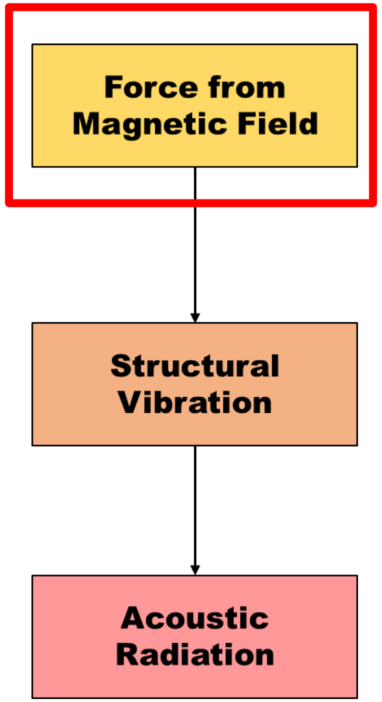

EMFF Part II: Impact of Armature / Windings

- The armature and current running through the coil windings impacts the magnitude of the total magnetic flux density and introduces the effect of the harmonics from the current waveform
- Re-shapes the magnetic flux density response given by the permanent magnets
- Relative recoil permeability of the permanent magnets is assumed to be unity (neodymium is ~1.05) - does not introduce any significant error into the calculation of the total field distribution since the armature reaction field is usually only around 10-20% of the magnitude of the open-circuit field [1]
- Outrunner electric motor with 3-phase windings, this results in an equation that can be numerically evaluated:

$$B_{R,W}(\phi, r, t) = \mu_0 \frac{3W}{\pi}\frac{1}{\delta}\sum_u I_u \sum_v \frac{1}{v} K_{sov} K_{dpv} F_v(r) \sin[up\omega_r t \pm v\phi + \theta_u],$$

$$where, F_v(r) = \delta \frac{v}{r}\left(\frac{r}{R_s}\right)^v \frac{1+\left(\frac{R_r}{r}\right)^{2v}}{1-\left(\frac{R_r}{R_s}\right)^{2v}},$$

$$and, v = p(6c - \{\pm\}u), c = \pm 1, \pm 2, \ldots, u = 1,5,7,11, \ldots, \quad harmonic\ orders,$$

Where W is number of turns per phase, δ is the effective airgap length, ω_r is the rotor angular velocity, I_u are the significant harmonics, K_{sov} is the slot opening factor, K_{dpv} is the winding distribution and pitch factor, and θ_u is the harmonic phase angle

(This equation is assessed for our case at $r = R_s + air\ gap\ length + magnet\ thickness$, which is the outer shell surface)

Example output of magnetic flux density due to PM field, armature windings, and slotting for 5A current

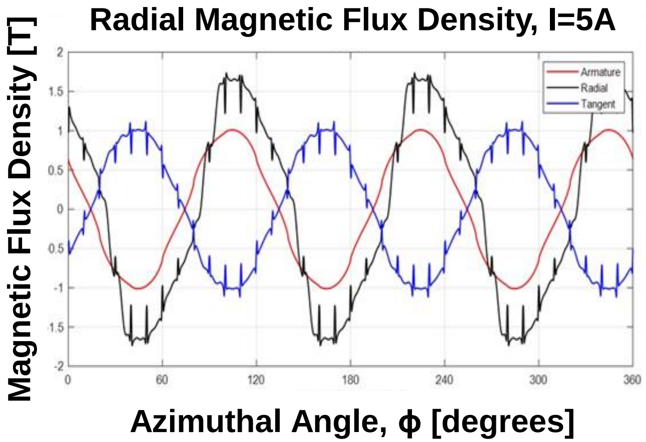

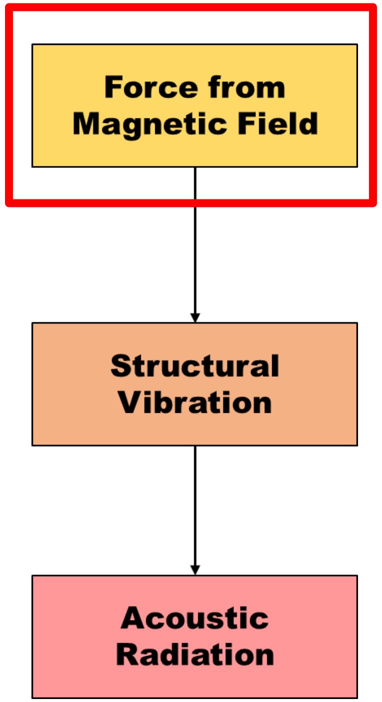

[1] Z. Q. Zhu and D. Howe, “Instantaneous magnetic field distribution in brushless permanent magnet dc motors, part II: Armature-reaction field,” IEEE Trans. Magn., pp. 136-143, 1993.

EMFF Part III: Slotting Effects

- Electric motor stator slotting introduces a relative permeance function that impacts the magnetic field distribution
- Slots cause interpolar flux leakage, therefore working point of the magnets will not be constant throughout their volume – magnetomotive force acting across the airgap will vary over a pole-arc
- Formulation assumes radial magnetization and linear demagnetization curve
- Currently working through implementing slotting effects part of the analytical tool
- Outrunner electric motor with 3-phase windings, this results in an equation that can be numerically evaluated:

$$\lambda(\phi, r, t) = \sum_{\mu=0}^{\infty} \widetilde{\Lambda}_{\mu}(r,t) \cos \mu Q_s(\phi + \phi_{sa}),$$

Where $\widetilde{\Lambda}_{\mu}(r,t)$ is a permeance function relating the slot height and air gap radial location, Q_s is total number of slots, and ϕ_{sa} is the half slot pitch angle for odd integers and 0 for even integers

(This equation is assessed for our case at $r = R_s + air\ gap\ length + magnet\ thickness$, which is the outer shell surface)

<u>Example output of magnetic flux density due to PM field and slotting only</u>

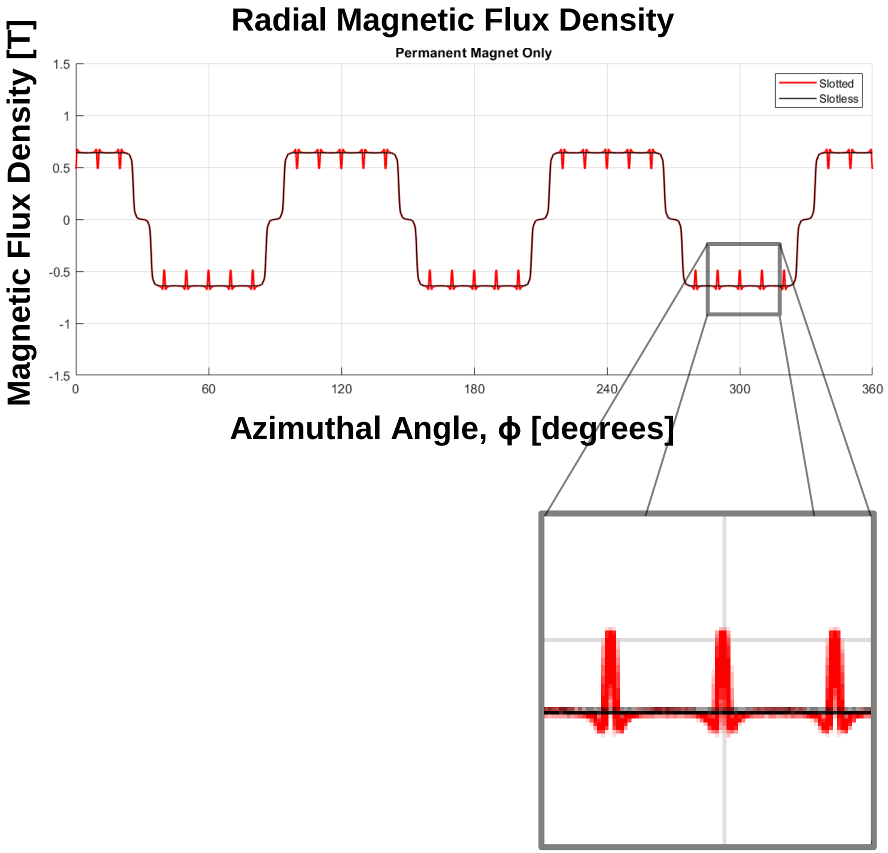

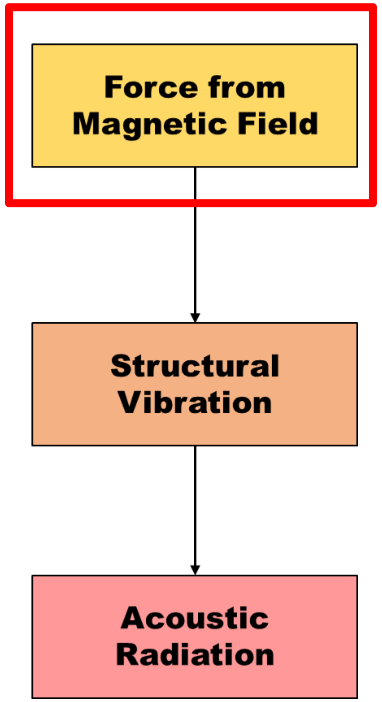

EMFF Model Example

Example input current waveform

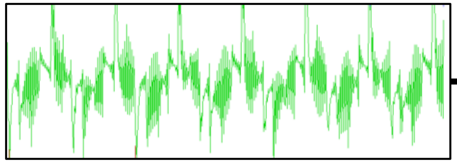

Electromagnetic forcing function [EMFF] tool (MATLAB)

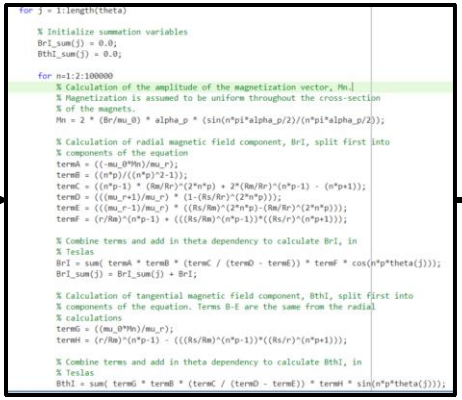

MATLAB

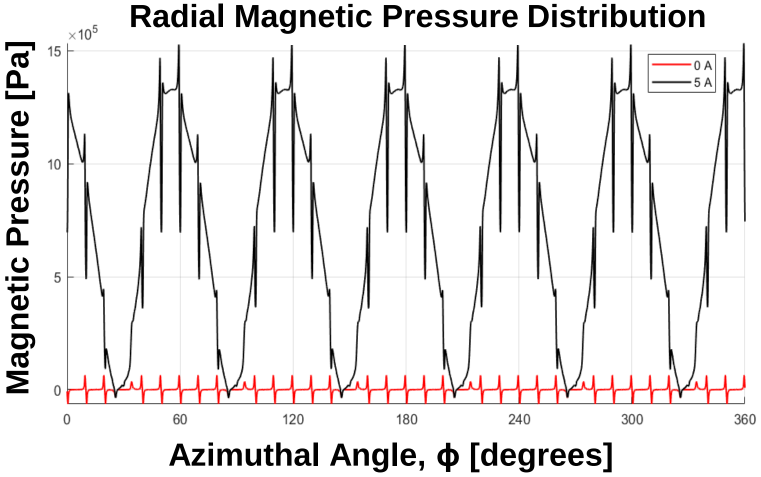

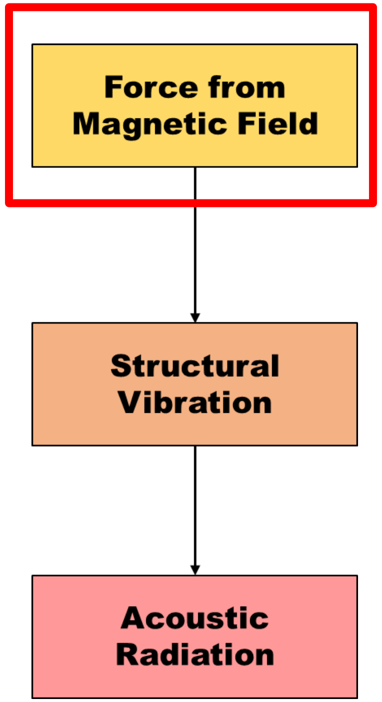

Input electric motor geometry

Parameters	Symb ol	Value
Number of pole pairs	$p\ [-]$	3
Number of slots	$Q_s\ [-]$	36
Stator outer radius	$R_s\ [m]$	$57.5\ 10^{-3}$
Permanent magnet thickness	$h\ [m]$	$2\ 10^{-3}$
Air gap length	$g\ [m]$	$0.5\ 10^{-3}$
Length	$L\ [m]$	$100\ 10^{-3}$
Magnet remanence	$B_r\ [T]$	0.82
Magnet arc/pole pitch ratio	$\alpha_p\ [-]$	0.865
Number of turns on each coil	$N\ [-]$	500
Rel. permeability of slot material	$\mu_r\ [-]$	1.07

$$F_R(\phi, t) = \frac{1}{2b}\int p_R dz$$

Output magnetic forces at vibrating surface and associated harmonics

To Structural Vibration Model

Electric Motor Noise Modeling Process

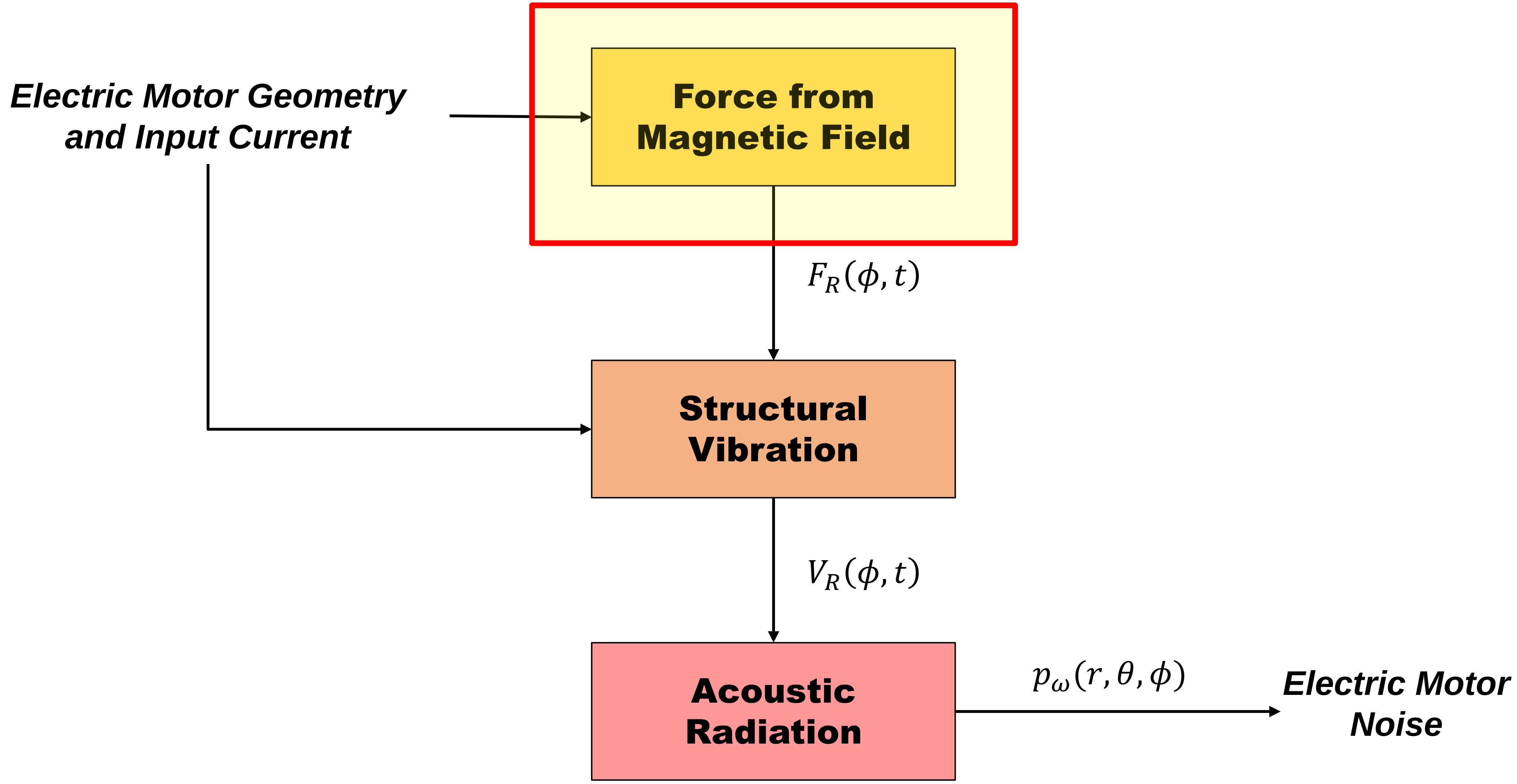

Vibration – Azimuthal, Axial Modes

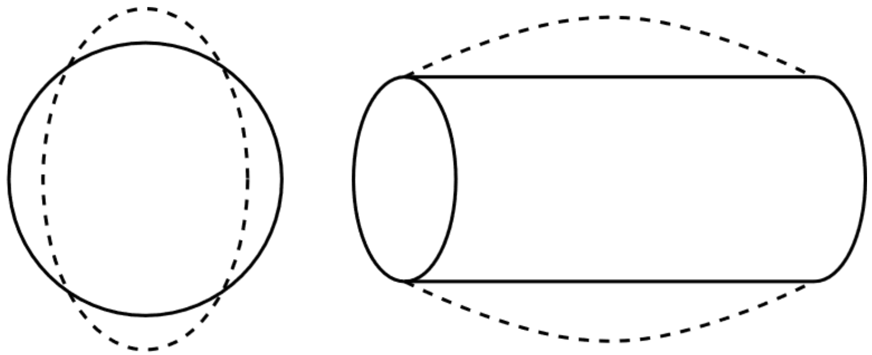

Azimuthal Mode Number M

Axial Mode Number N

When aspect ratio (D/L) > 1, N is 1 for audible frequencies

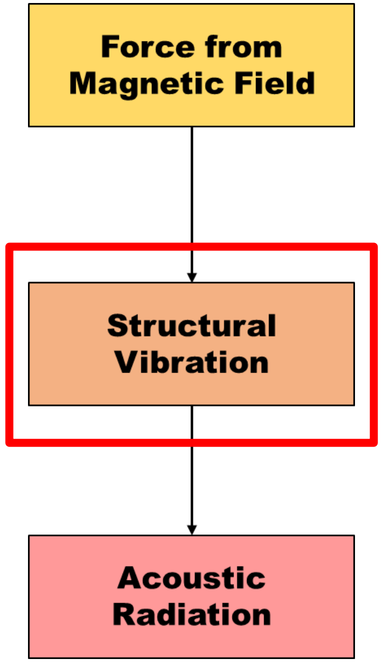

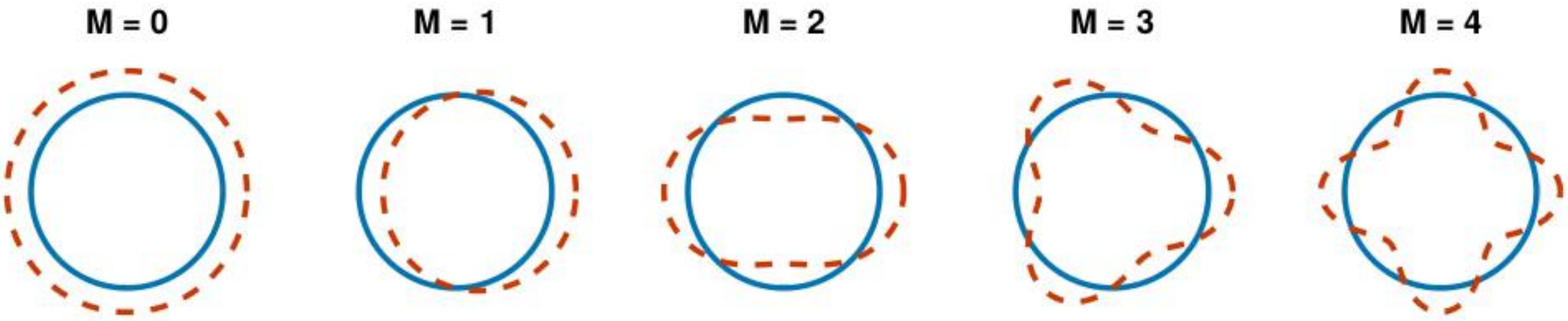

Overall Process – Low Fidelity FEA Model, Anchored in Experiments

<u>Simplified Model Development</u>

- Validate high fidelity models against experimental results
- Create simplified geometry
- Use simplified geometry to create a synthetic dataset
- Curve fit the synthetic dataset

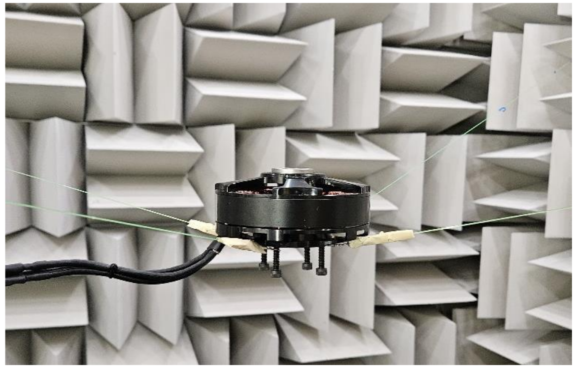

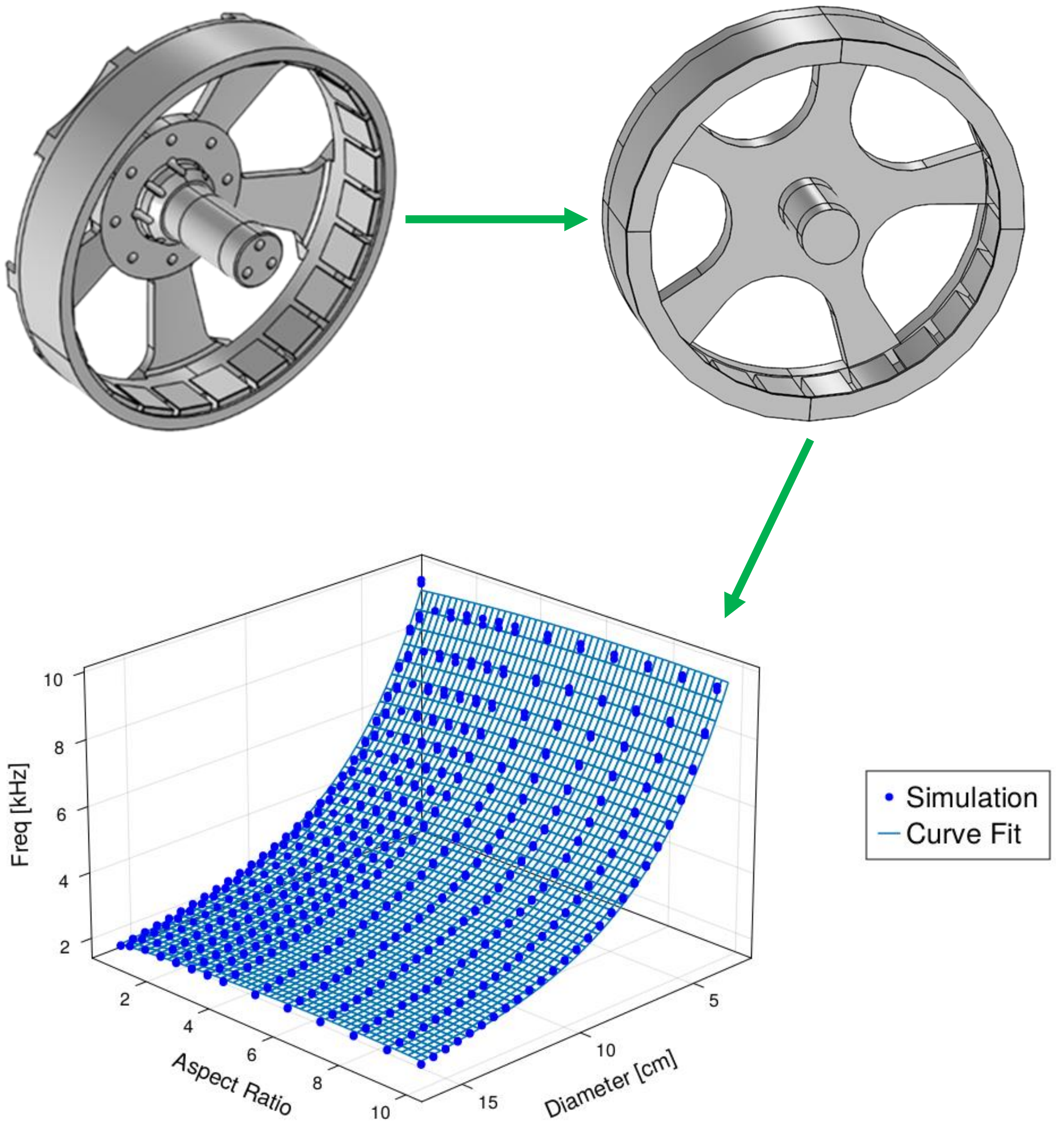

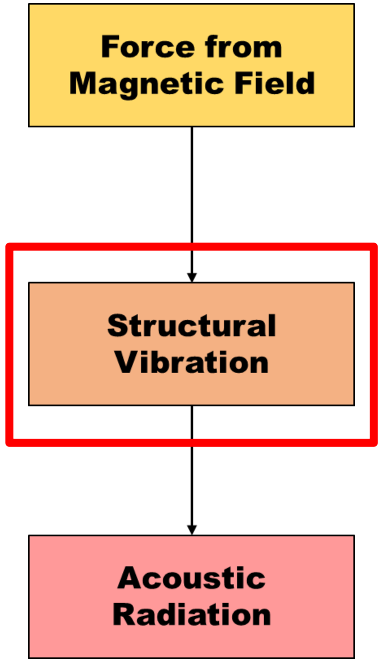

Eigenmode Problem

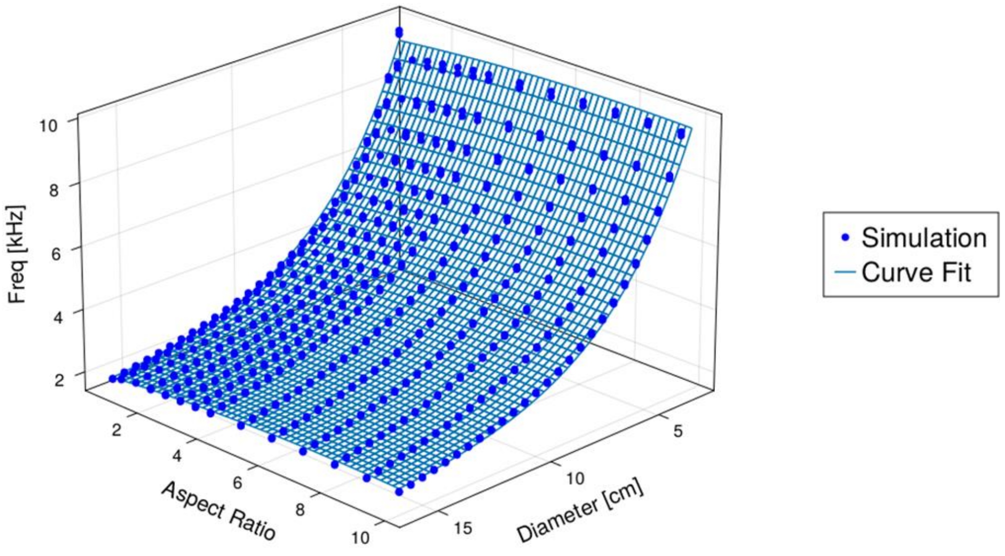

Mode Shape (m,n)	Label	Predicted Freq [Hz]	Experimentally Measured Freq [Hz]
1,1	a	935	
2,1	b	3515	2971
1,1	c	6411	5942
3,1	d	6676	6919
0,1	e	7023	
0,1	f	8382	
4,1	g	8841	

Eigenfrequency Prediction

- For each eigenmode a curve fit over the range of motor geometries is created
- Resulting eigenfrequency predictions are a good match to experimental measurements

See Paper: *An Initial Electric Motor Rotor Vibration Model,* AIAA 2024-2302

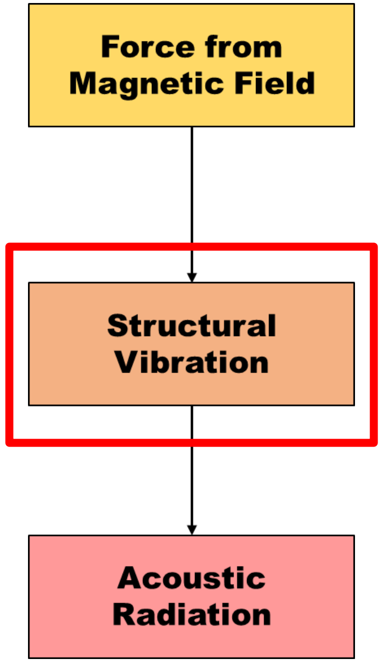

Forced Vibration Problem - 1

- Radial force is applied. The forcing varies sinusoidally at a given frequency and azimuthally to correspond to a given mode shape, *m*.

- The applied forcing results in a corresponding surface displacement. The maximum displacement at any point on the surface is taken as the vibration amplitude.

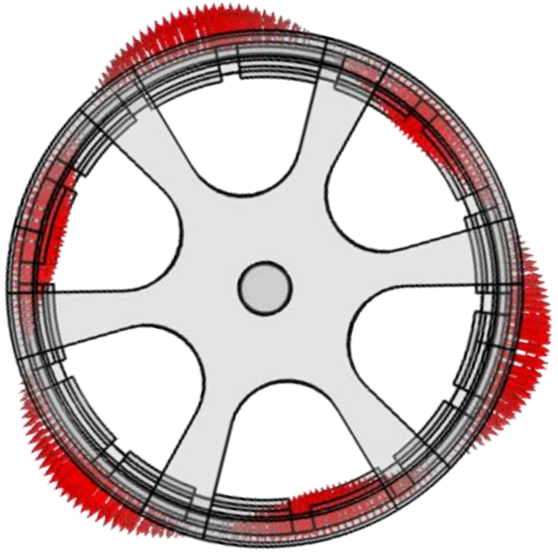

m = 3

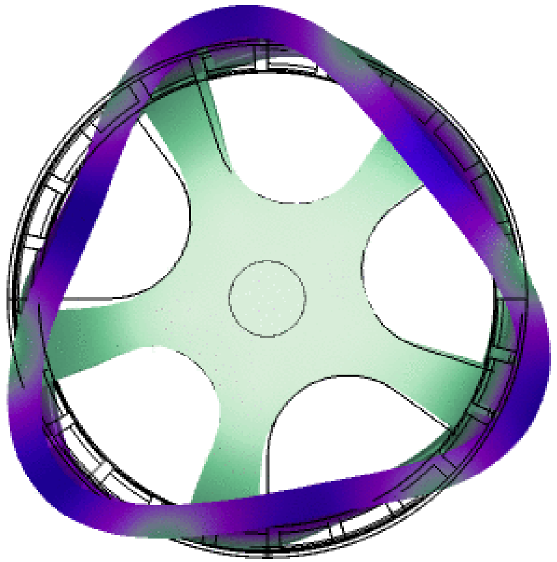

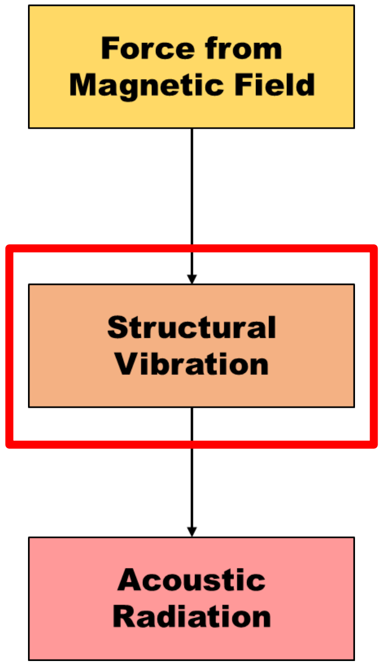

Forced Vibration Problem - 2

- Repeating this process for a range of motor geometries, frequencies creates a group of curves

- Motor diameters 50-100mm and height from 15-35mm

- Each curve can be normalized by peak frequency and peak amplitude

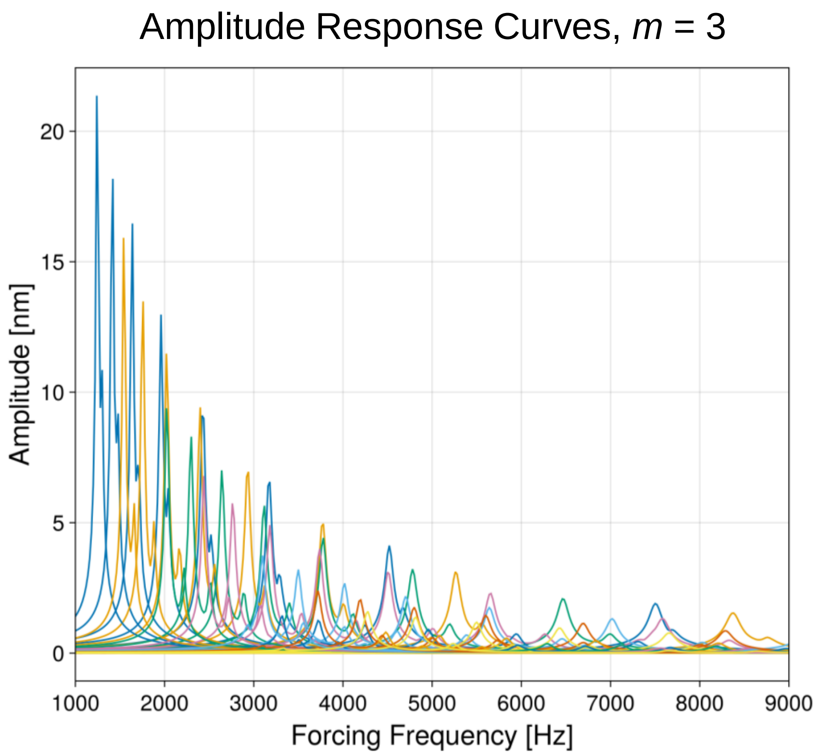

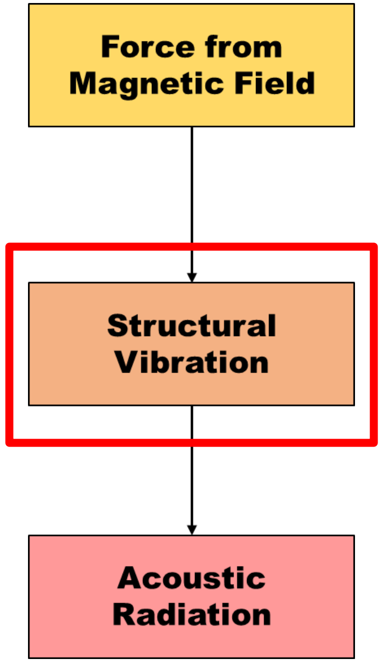

Forced Vibration Problem - 3

- When normalized across the range of geometries the data collapses well

- A curve fit is applied

- Note that the curve shape closely matches the analytical solution to the forced damped SDOF oscillator

- Using this fitted curve, the forcing frequency, predicted eigenfrequency, and peak amplitude we can dimensionalize and generate a peak surface displacement prediction

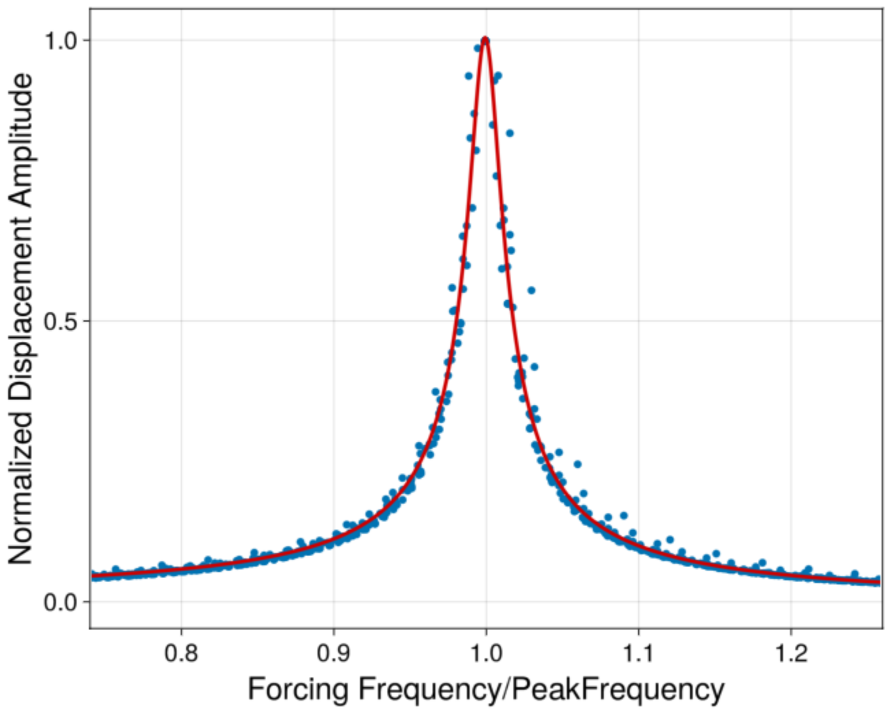

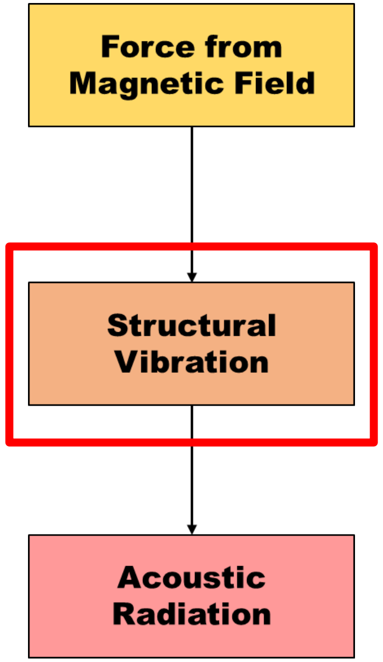

Forced Vibration Problem - 4

- Eigenfrequency prediction is already complete
- The eigenfrequency displacement amplitude is well behaved as motor geometry varies and can similarly be predicted by interpolation or curve fit
- For kW range of motors of interest, twenty distinct modes are needed to sufficiently capture the displacement

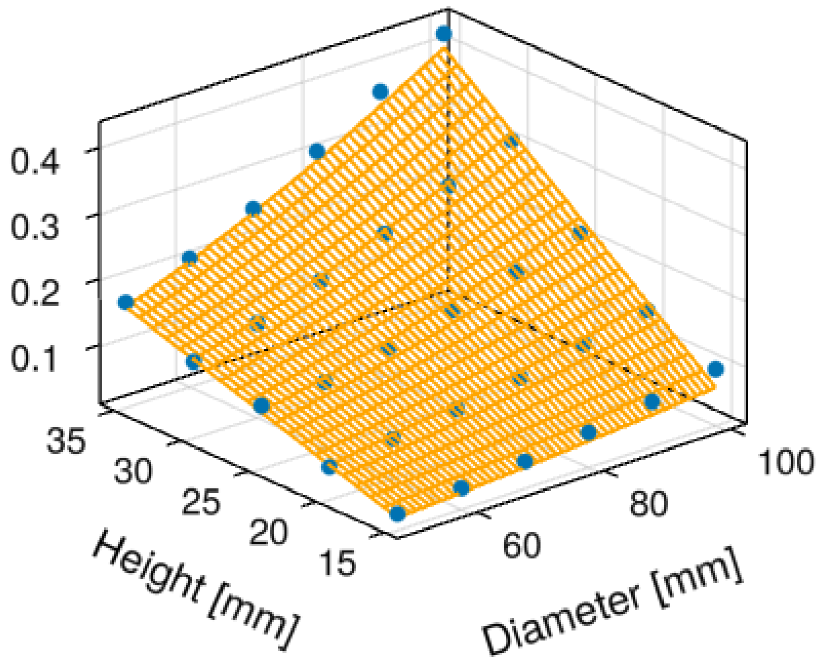

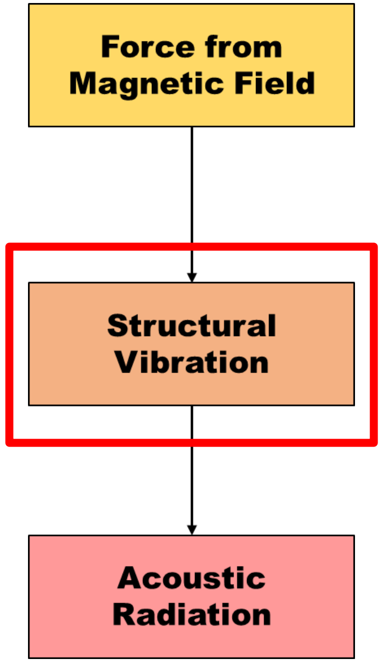

Electric Motor Noise Modeling Process

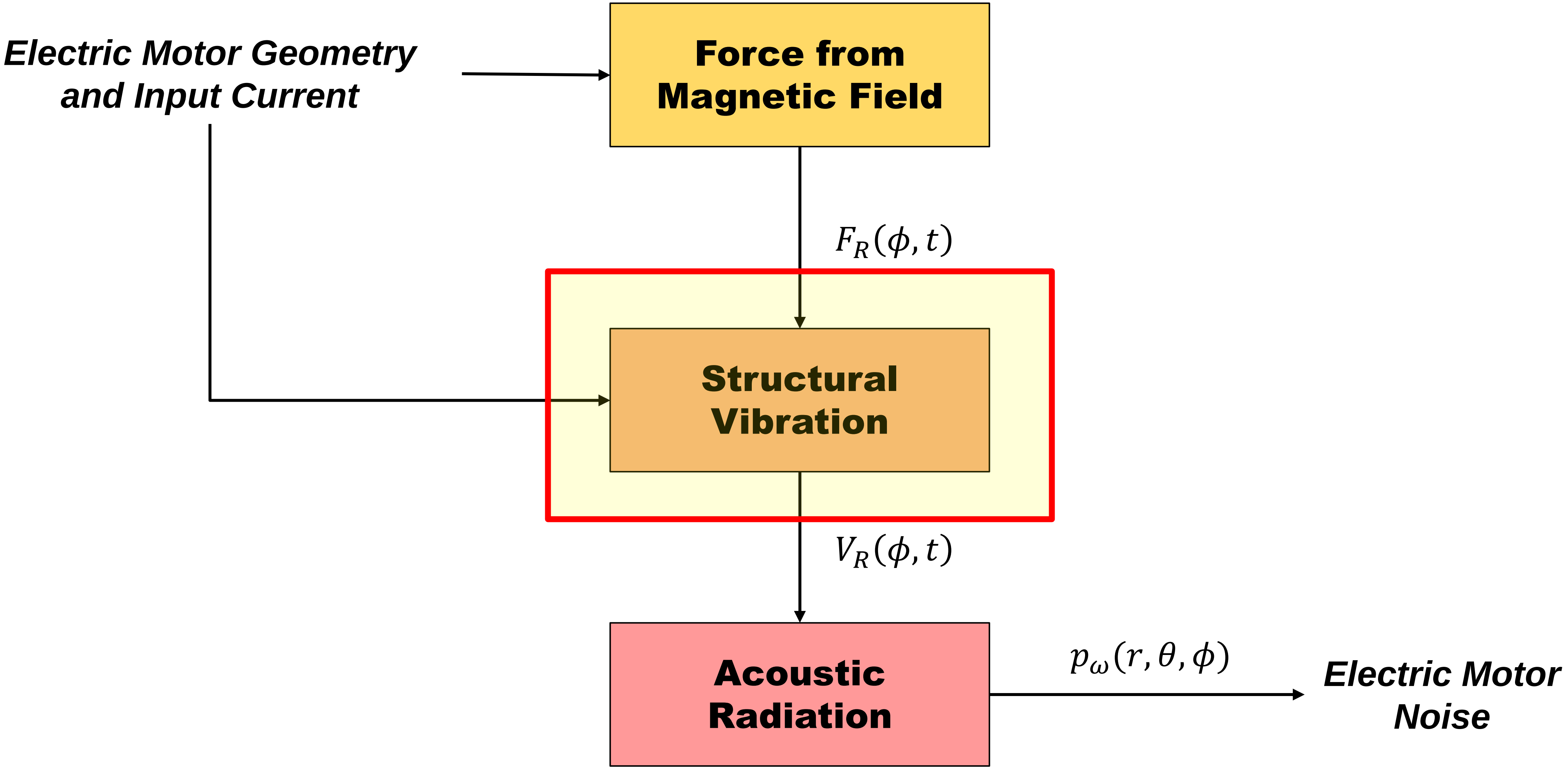

Previous Approaches

- Infinite cylinder solution ✓
  - JASA, vol. 24, pp. 46 – 49 (1952)
  - Textbook solution
  - Impact of finite length not captured
  - Rotation not captured
- Finite cylinder, non-rotating, least squares Method of Weighted Residuals (MWR) solution ✓
  - JASA, vol. 36, pp. 2316 – 2322 (1964)
  - Results in matrix inversion of poorly conditioned matrix
    - Decomposition and conditioning doesn't change poorly conditioned matrix
    - Can usually get a solution if using limited number of terms
  - Rotation not captured
- Finite cylinder, rotating, Galerkin (MWR) solution
  - JSV, vol. 428, pp. 59 – 71 (2018)
  - Intricate implementation over infinite domain

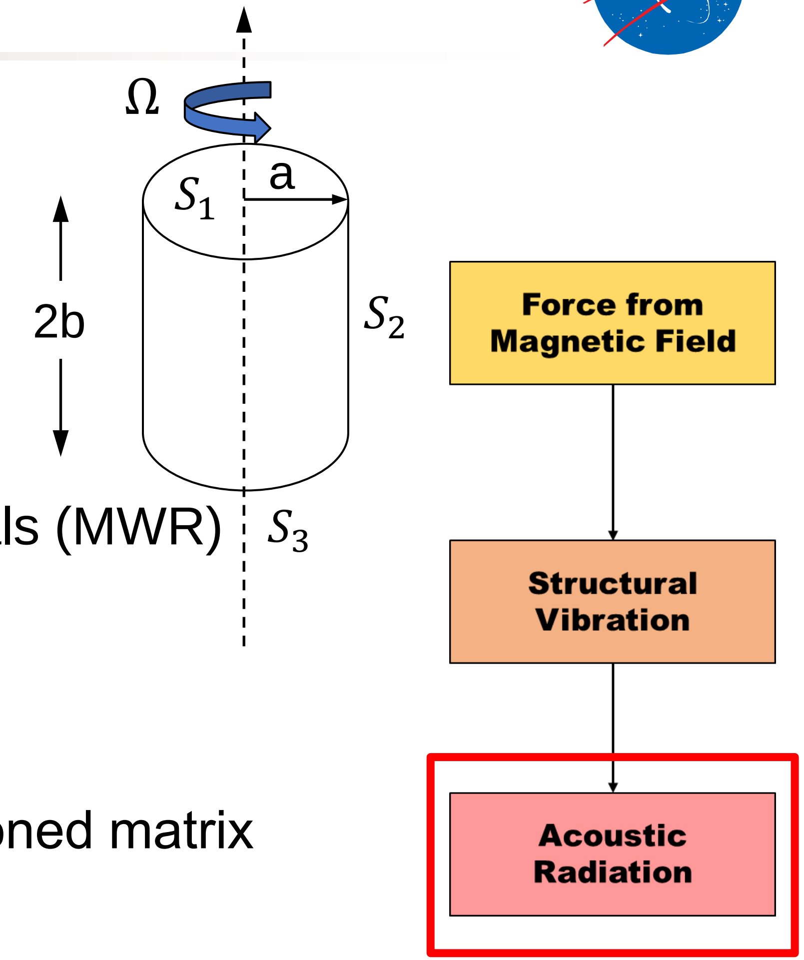

The Wave Equation and Boundary Conditions

- We seek a solution to the wave equation (in spherical coordinates)
  - $\nabla^2\psi - \frac{1}{c^2}\frac{\partial^2\psi}{\partial t^2} = 0, \quad \psi =$ Velocity Potential
- With the radial displacement on a cylindrical surface (S_2) given by
  - $w_R(\phi, z, t) = [A\sin(m\phi - m\Omega t) + B\cos(m\phi - m\Omega t)]\Phi_n(z)e^{i\omega t}$ — 1 for now ($\Phi_n(z)$) — JSV (2018)
  - ω is the vibration frequency in the rotating frame of reference
- Boundary Conditions
  - $\left.\frac{\partial\psi}{\partial n}\right|_{S_1,S_3} = 0$ JASA (1964)
  - $\left.\frac{\partial\psi}{\partial n}\right|_{S_2} = \left.\frac{Dw_R}{Dt}\right|_{S_2} = \left.\frac{\partial w_R}{\partial t} - \Omega\frac{\partial w_R}{\partial\phi}\right|_{S_2}$ JSV (2018) JASA (1964) for Ω = 0
- Reformat problem
  - $w_R(\phi, z, t) = C\_e^{im\phi}e^{i(\omega - m\Omega)t}$ (for backward rotating)
  - $\left.\frac{\partial\psi}{\partial n}\right|_{S_2} = i(\omega - 2m\Omega)C\_e^{im\phi}e^{i(\omega-m\Omega)t} = De^{im\phi}e^{i(\omega-m\Omega)t}$
  - For given m, ω, Ω

    $D = i(\omega - 2\mathrm{m}\Omega)C\_ = constant$

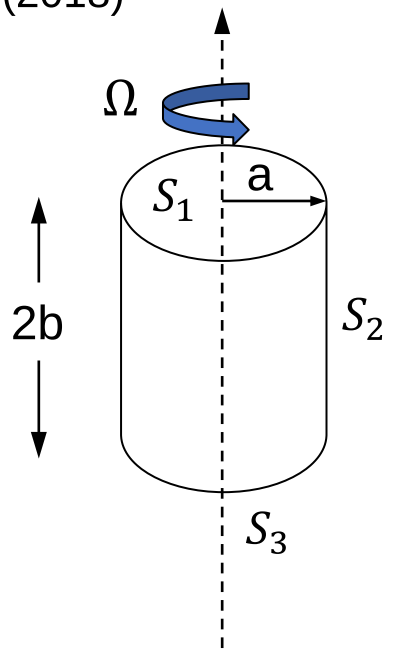

JASA (1964) for Ω = 0

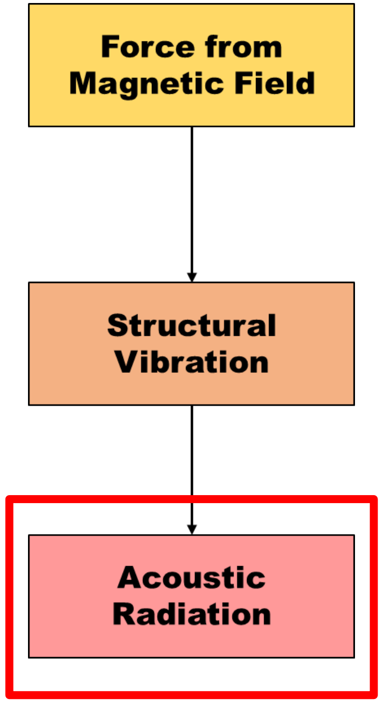

General Form of the Solution

- Assume a general form of solution to the wave equation
  - $\psi = \tilde{\psi}(r, \theta, \phi) e^{i(\omega - m\Omega)t}$
- Insert general solution in wave equation
  - $\nabla^2 \tilde{\psi} + \left(\frac{\omega - m\Omega}{c}\right)^2 \tilde{\psi} = 0$

  or

  - $\nabla^2 \tilde{\psi} + \tilde{k}^2 \tilde{\psi} = 0$ ***Helmholtz Equation***
- Now we can use solutions to the finite cylinder with no rotation for the rotating cylinder
- General solution for Helmholtz Equation
  - $\tilde{\psi}(\vec{r}) = \sum_{l=0}^{\infty} a_{lm} \tilde{\psi}_{lm}(\vec{r}) = \sum_{l=0}^{\infty} a_{lm} h_l^{+}(\tilde{k}r) P_l^m(\cos\theta) e^{im\phi}$

  h_l^{+} = outgoing spherical Hankel function of order l

  P_l^m = associated Legendre polynomial of degree l and order m
- We now have a problem of undetermined coefficients; any Method of Weighted Residuals technique can be used to determine the coefficients

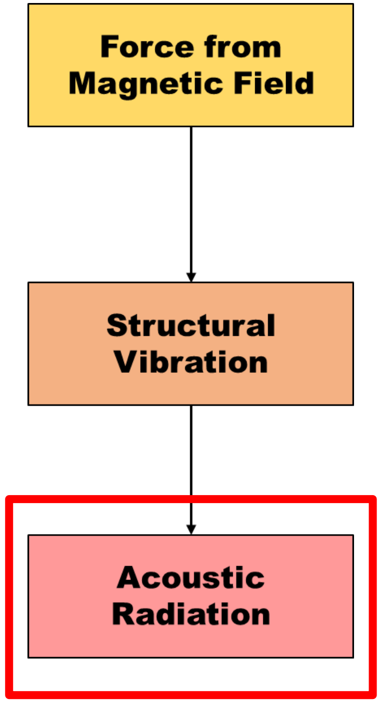

Least Squares Solution

r = 10
a = 1
b = 1
$\tilde{k}$ = 2
m = 0

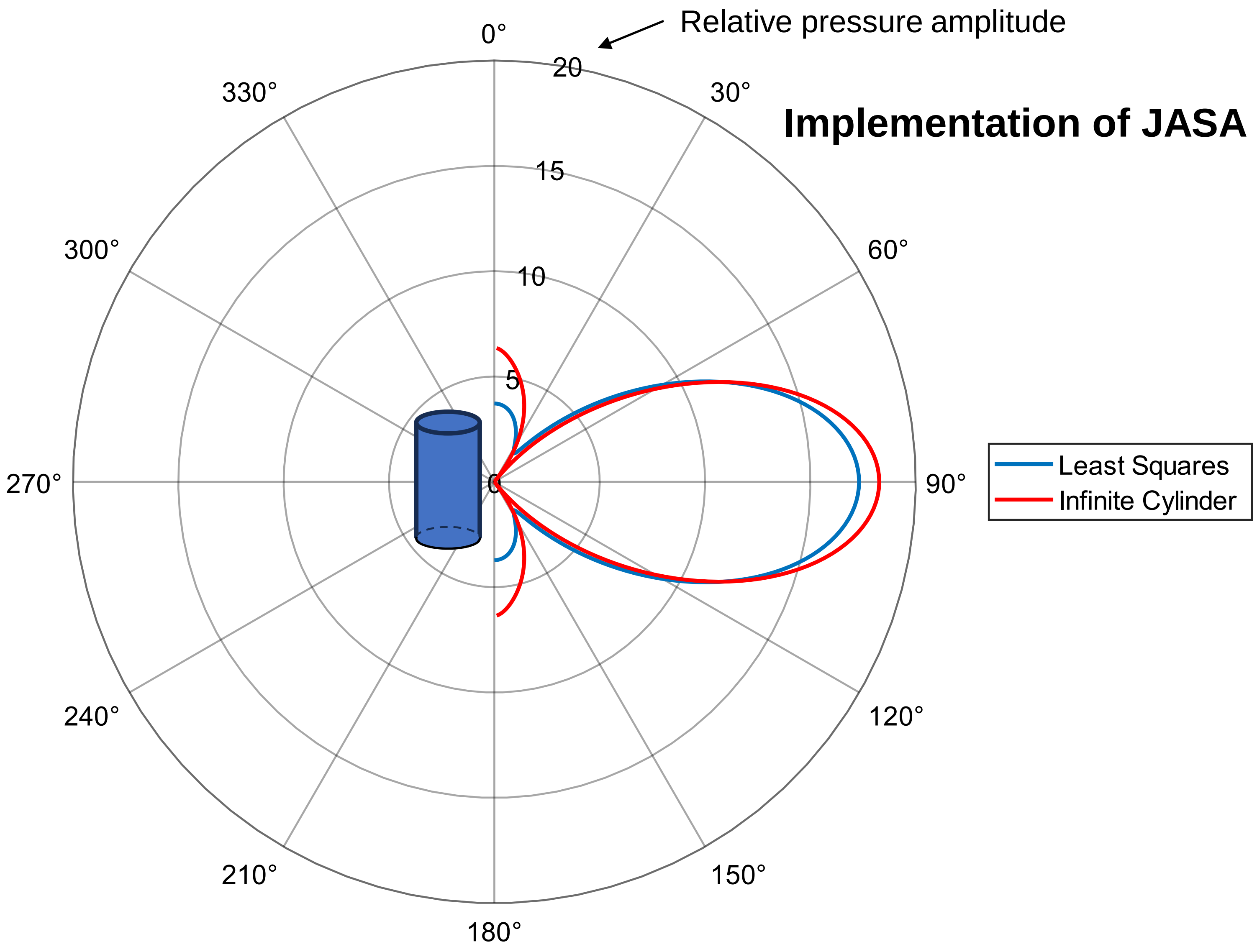

Implementation of JASA (1964)

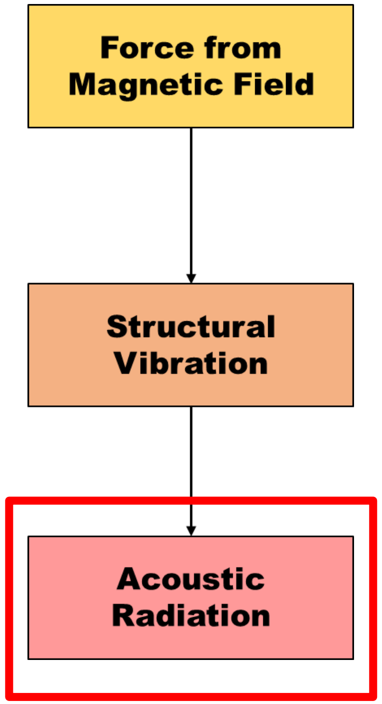

Galerkin Solution

- Require residual to be orthogonal to basis functions
  - $\int\left(\nabla^2\tilde{\psi}+\tilde{k}^2\tilde{\psi}\right)\tilde{\psi}_{lm}^{*}dV=0$
- In the weak formulation, the basis functions do not satisfy the boundary conditions so you must use Gauss' Divergence theorem to incorporate boundary conditions
  - $\int\left[\nabla\tilde{\psi}\cdot\nabla\tilde{\psi}_{lm}^{*}-\tilde{k}^2\tilde{\psi}\tilde{\psi}_{lm}^{*}\right]dV=\oint\frac{\partial\tilde{\psi}}{\partial n}\cdot\tilde{\psi}_{lm}^{*}dS$
  - Two surfaces bound the volume
    - ➢ Inner surface – oscillating cylindrical surface
    - ➢ Outer surface - $r\rightarrow\infty$ and $\psi\rightarrow 0$ complicates one of the volume integrals
- Coefficients are determined from
  - $\sum_{j=0}^{N}a_{jm}\left[\tilde{k}^2P1_{lj}H1_{lj}+P2_{lj}H2_{lj}+m^2P3_{lj}H2_{lj}-\tilde{k}^2P1_{lj}H3_{lj}\right]=-2B_l$

$$H1_{lj}=\int r^2h_j^{+'}(\tilde{k}r)h_l^{+'*}(\tilde{k}r)dr \qquad P1_{lj}=\int\sin\theta\,P_l^m(\cos\theta)P_j^m(\cos\theta)d\theta,$$

$$H1_{lj}=\int r^2h_j^{+'}(\tilde{k}r)h_l^{+'*}(\tilde{k}r)dr \qquad P2_{lj}=\int(\sin\theta)^3\,P_l^{m'}(\cos\theta)P_j^{m'}(\cos\theta)d\theta$$

$$H3_{lj}=\int r^2h_j^{+}(\tilde{k}r)h_l^{+*}(\tilde{k}r)dr \qquad P3_{lj}=\int P_l^m(\cos\theta)P_j^m(\cos\theta)\frac{d\theta}{\sin\theta}$$

$$B_l=C_{\omega m\Omega}\int_{\theta_0}^{\pi/2}P_l^m(\cos\theta)h_l^{+*}\left(\frac{\tilde{k}a}{\sin\theta}\right)d\theta$$

most, but not all, integrals have analytical solutions

- In the process of implementing the solution

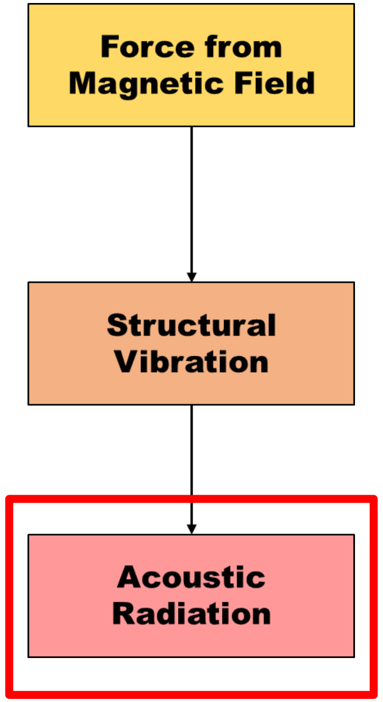

Summary

- Modeling effort consists of three distinct components
  - Electromagnetic forcing
  - Structural vibrations
  - Acoustic radiation
- Permanent magnet and windings models of the EMFF tool completed; slotting model under development
- Individual structural vibration model components validated against experiment; full unified structural model being implemented
- Implementation of the Galerkin model for acoustic radiation is in progress; expected to have better numerical properties than least square model
- On track to complete initial combined system-level toolchain by end of CY 2024

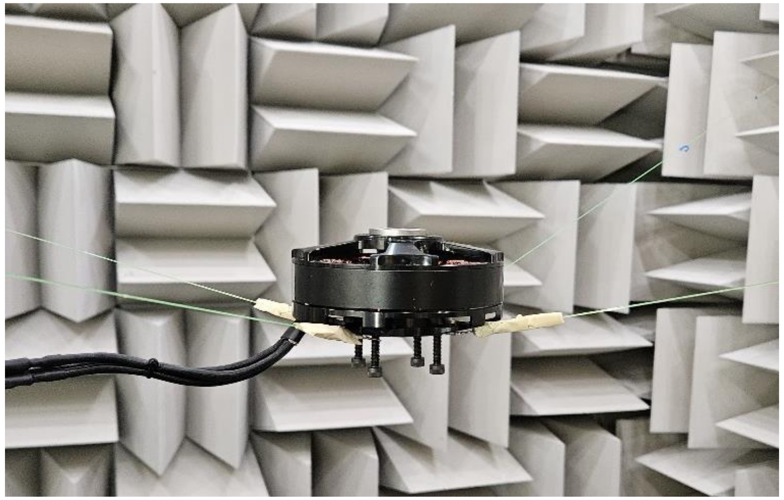

Electric motor noise test in ATL

Impact / Significance:
Enable system-level trade-off studies at early design stage of AAM vehicles